Molecular Pharmacology Fast Forward. Published on October 8, 2020 as DOI: 10.1124/molpharm.120.000070
This article has not been copyedited and formatted. The final version may differ from this version.

GZD824 inhibits GCN2 and sensitizes cancer cells to amino acid starvation stress

Yu Kato[a,b], Kazuhiro Kunimasa[a], Mizuki Takahashi[a,b], Ayaka Harada[c], Ikuko Nagasawa[a], Masanori Osawa[c], Yoshikazu Sugimoto[b] and Akihiro Tomida[a]

[a] Cancer Chemotherapy Center, Japanese Foundation for Cancer Research, 3-8-31, Ariake, Koto-ku, Tokyo 135-8550, Japan

[b] Division of Chemotherapy, Faculty of Pharmacy, Keio University, 1-5-30, Shibakoen, Minato-ku, Tokyo 105-8512, Japan.

[c] Division of Physics for Life Functions, Faculty of Pharmacy, Keio University, 1-5-30, Shibakoen, Minato-ku, Tokyo 105-8512, Japan.

Molecular Pharmacology Fast Forward. Published on October 8, 2020 as DOI: 10.1124/molpharm.120.000070
This article has not been copyedited and formatted. The final version may differ from this version.

Running title: Identification of GZD824 as GCN2 inhibitor

Correspondence to: Akihiro Tomida

Email: akihiro.tomida@jfcr.or.jp

TEL: +81-3-3570-0514

Cancer Chemotherapy Center, Japanese Foundation for Cancer Research, 3-8-31,

Ariake, Koto-ku, Tokyo 135-8550, Japan

Number of text pages：32

Numbers of tables: 0

Numbers of figures: 6

Numbers of references: 28

Number of words of Abstract: 156

Number of words of Introduction: 432

Number of words of Discussion: 759

List of Abbreviations

GCN2: general control non-derepressible 2

ATF4: activating transcription factor 4

eIF2α: eukaryotic initiation factor 2α

ISR: integrated stress response

PERK: protein kinase-like endoplasmic reticulum kinase

Molecular Pharmacology Fast Forward. Published on October 8, 2020 as DOI: 10.1124/molpharm.120.000070
This article has not been copyedited and formatted. The final version may differ from this version.

Molecular Pharmacology Fast Forward. Published on October 8, 2020 as DOI: 10.1124/molpharm.120.000070
This article has not been copyedited and formatted. The final version may differ from this version.

Abstract

Eukaryotic initiation factor 2α kinase general control non-derepressible 2 (GCN2) drives cellular adaptation to amino acid limitation by activating the integrated stress response that induces activating transcription factor 4 (ATF4). Here, we found that a multi-kinase inhibitor, GZD824, which we identified using a cell-based assay with ATF4 immunostaining, inhibited the GCN2 pathway in cancer cells. Indeed, GZD824 suppressed GCN2 activation, eIF2α phosphorylation, and ATF4 induction during amino acid starvation stress. However, at lower non-suppressive concentrations, GZD824 paradoxically stimulated eIF2α phosphorylation and ATF4 expression in a GCN2-dependent manner under unstressed conditions. Such dual properties conceivably arose from a direct effect on GCN2, as also observed in a cell-free GCN2 kinase assay and shared by a selective GCN2 inhibitor. Consistent with the GCN2 pathway inhibition, GZD824 sensitized certain cancer cells to amino acid starvation stress similarly to ATF4 knockdown. These results establish GZD824 as a multi-kinase GCN2 inhibitor and may enhance its utility as a drug under development.

Molecular Pharmacology Fast Forward. Published on October 8, 2020 as DOI: 10.1124/molpharm.120.000070
This article has not been copyedited and formatted. The final version may differ from this version.

Significance statement

GZD824, as a direct GCN2 inhibitor, suppresses activation of the integrated stress response during amino acid limitation, while it paradoxically stimulates this stress-signaling pathway at lower non-suppressive concentrations. The pharmacological activity, we identified herein, will provide the basis for the use of GZD824 to elucidate the regulatory mechanisms of GCN2 and to evaluate the potential of the GCN2-ATF4 pathway as a target for cancer therapy.

Molecular Pharmacology Fast Forward. Published on October 8, 2020 as DOI: 10.1124/molpharm.120.000070
This article has not been copyedited and formatted. The final version may differ from this version.

1. Introduction

The integrated stress response (ISR) plays an important role in cellular adaptation to various stress conditions (Harding et al., 2003; Ye et al., 2010; Harding et al., 2010; Dang et al., 2012). Under distinct stress conditions, ISR is activated by four eukaryotic initiation factor 2α (eIF2α) kinases: general control non-derepressible 2 (GCN2), protein kinase-like endoplasmic reticulum kinase (PERK), double-stranded RNA-dependent kinase, and heme-regulated inhibitor (Quiros et al., 2016). These eIF2α kinases commonly phosphorylate eIF2α at S51, thereby reducing general protein synthesis. However, specific mRNAs with an upstream open reading frame, such as *ATF4*, are selectively translated by delaying translation reinitiation via eIF2α phosphorylation (Vattem et al., 2004; Lu et al., 2004). ATF4, a key transcription factor for stress adaptation, subsequently drives transcription of genes involved in processes such as protein folding, amino acid metabolism, and autophagy (Zhu et al., 2019).

Among the eIF2α kinases, GCN2 is activated in response to amino acid starvation and plays a central role in cellular adaptation to tumor microenvironments (Qiu et al., 1998). Within tumors, cancer cells are often undergo amino acid deprivation, partly because abnormal proliferation increases the need for amino acids to produce proteins, lipids, and nucleic acids, and partly because insufficient and disorganized formation of blood vessels leads to a supply shortage of amino acids. Thus, GCN2 can be important for cancer cell survival and tumor development, and consistently, knockout of GCN2 or ATF4 has been shown to decrease tumor growth *in vivo* (Ye et al., 2010). In addition, the GCN2 arm of the ISR has been recently shown to protect cancer cells from intrinsic stress induced by the *c-Myc* oncogene by inducing adaptive gene expression and limiting Myc overexpression (Tameire et al., 2019; Schmidt et al., 2019).

Molecular Pharmacology Fast Forward. Published on October 8, 2020 as DOI: 10.1124/molpharm.120.000070
This article has not been copyedited and formatted. The final version may differ from this version.

GCN2 can also be involved in resistance to cancer chemotherapy, because sensitization to anti-tumor agent L-asparaginase is elicited by GCN2 inhibition in cancer cells that express asparagine synthetase at low levels (Nakamura et al., 2018).

It has been suggested that the GCN2-mediated ISR pathway provides promising targets for cancer therapy, but there are few GCN2 inhibitors available. In this study using a kinase inhibitor library, we screened compounds that inhibit the GCN2 pathway. As a result, we successfully identified GZD824, a known BCR-ABL inhibitor (Ren et al., 2013), which prevents GCN2 pathway activation during amino acid starvation stress. We further found that GZD824 directly inhibited GCN2 kinase activity and sensitized certain cancer cell lines to amino acid starvation stress. Our findings from this exploratory study indicate that GZD824 is useful to investigate the role of GCN2 in cellular stress adaptation as a target for cancer therapy.

Molecular Pharmacology Fast Forward. Published on October 8, 2020 as DOI: 10.1124/molpharm.120.000070
This article has not been copyedited and formatted. The final version may differ from this version.

2. Material and Methods

2.1 Cell culture and regents

Human fibrosarcoma cell line HT1080 and non-small cell lung cancer cell lines NCI-H460 and A549 were obtained from the American Type Culture Collection (Manassas, VA, USA). HT1080, NCI-H460 and A549 cells were maintained in RPMI-1640 (Wako Pure Chemical Industry, Osaka, Japan) with 10% fetal bovine serum (Merck, Burlington, MA, USA) as described previously (Saito et al., 2009). All the cells were checked to be mycoplasma free. GZD824 (Selleck Chemicals, Houston, TX, USA), GCN2iB (MedChemExpress, Monmouth Junction, NJ, USA), GSK2656157 (Merck), halofuginone (Merck), tunicamycin (Nacalai Tesque, Kyoto, Japan) and thapsigargin (Wako, Osaka, Japan) were dissolved in DMSO as stock solutions (final concentration was less than 0.5% solvent). Histidinol (Merck) was dissolved in sterilized distilled water.

2.2 RNAi

Silencing of human *GCN2, PERK,* and *ATF4* expression was performed using ON-TARGETplus SMARTpool siRNAs (*GCN2*: L-005314, *PERK*: L-004883-00, *ATF4*: L-005125; GE Healthcare, Little Chalfont, UK) or Silencer Select siRNA (*ATF4*: s1702; Thermo Fisher Scientific, Waltham, MA, USA) with Lipofectamine RNAiMAX transfection reagent (Thermo Fisher Scientific). On TARGETplus SMARTpool and Silencer Select siRNAs were used at 20 and 5 nM, respectively. Cells were transfected with each siRNA according to the manufacturers' reverse transfection protocol.

2.3 Immunofluorescence staining

Cells were seeded in a 96-well black plate. The cells were treated with reagents at the indicated concentration and time. The cells were fixed in 4% paraformaldehyde for 15

Molecular Pharmacology Fast Forward. Published on October 8, 2020 as DOI: 10.1124/molpharm.120.000070
This article has not been copyedited and formatted. The final version may differ from this version.

min and then permeabilized with 0.3% Triton X-100 in 4% BSA-PBS for 1 h. The cells were incubated with an anti-ATF4 antibody (#11815) (Cell Signaling Technology, Beverly, MA, USA) in 1% BSA-PBS overnight at 4 °C. Then, the primary antibody was reacted with an anti-rabbit IgG secondary antibody conjugated with Alexa Fluor-488 (Thermo Fisher Scientific) in 1% BSA-PBS for 1 h. The nucleus was counterstained with Hoechst 33342 (Thermo Fisher Scientific). Fluorescence images were obtained by an IN CELL ANALYZER 6000 (GE Healthcare, Little Chalfont, UK). Quantification of the nuclear ATF4 intensity was performed using IN CELL Developer Toolbox software (GE Healthcare).

2.4 Immunoblot analysis

Immunoblot analysis was performed as described previously (Saito et al., 2009). Briefly, cell lysates were prepared using SDS lysis buffer (62.5 mM Tris-HCl, pH 6.8, 2% SDS, 50 mM dithiothreitol, and 10% glycerol). Protein concentrations were determined using a Bio-Rad protein assay (Bio-Rad, Hercules, CA, USA). Protein samples were subjected to sodium dodecyl sulfate-polyacrylamide gel electrophoresis and subsequently transferred onto a nitrocellulose membrane. Membranes were incubated with primary antibodies against phospho-GCN2 (Thr899) (ab75836), PERK (ab65142) and eIF2S1 (ab5369) (Abcam, Cambridge, UK); GCN2 (#3302), phosphor-eIF2α (Ser51) (#3398), ATF4 (#11815) and RPS3 (#9538) (CST). After washing, the membranes were further incubated with appropriate secondary antibodies [Anti-Mouse IgG, HRP-Linked Whole Ab Sheep or Anti-Rabbit IgG, HRP-Linked Whole Ab Donkey (GE Healthcare)]. The specific signals were detected using Western Lighting plus ECL (Perkin Elmer, Waltham, MA, USA).

2.5 In vitro kinase assay

Molecular Pharmacology Fast Forward. Published on October 8, 2020 as DOI: 10.1124/molpharm.120.000070
This article has not been copyedited and formatted. The final version may differ from this version.

Eight μL of recombinant GCN2 protein (active; final concentration: 30 nM; SignalChem, Richmond, Canada) in reaction buffer (20 mM Hepes, pH 7.4, 5 mM $MgCl_2$, and 1 mM dithiothreitol) was preincubated with 0.2 μL of GZD824, dasatinib, or GCN2iB for 60 min at 30 °C. Then, GCN2 was incubated with 12 μL of 2 mM ATP (Sigma) and recombinant eIF2α (final concentration: 160 nM; SignalChem) for 3 h at 30 ℃. These samples were mixed with SDS lysis buffer (250 mM Tris HCl, pH 6.8, 8% SDS, 40% glycerol, 0.16% bromophenol blue, and 20% 2-mercaptoethanol) and boiled at 100 °C for 15 min. The samples were then subjected to immunoblot analysis as described in 2.4. The immunoblots were quantified using ImageJ (http://rsbweb.nih.gov/ij/) under the Gel Analysis Tool.

2.6 Structural comparison and preparation of a docking model of the GCN2-GZD824 complex

A docking model of the GCN2-GZD824 complex was prepared using coordinates of the GCN2-KAV (PDB ID; 6N3L) and ABL-AP24534 (PDB ID; 3OXZ) complexes. First, subunit A of the GCN2-KAV complex was superposed on subunit A of the ABL-AP24534 complex with the SSM-Superpose routine of Coot (Emsley et al., 2004; Krissnel et al., 2004), resulting in the root-mean-square deviation of 1.81Å. We confirmed that KAV and AP24534 in the complex structure were superposed well, and then replaced the coordinates of KAV in the GCN2-KAV complex with those of the superposed AP24534. Second, we replaced the imidazo[1,2-b]pyridazin group of AP23534 to the 1*H*-pyrazolo[3,4-b]pyridine group to obtain GZD824. All molecular graphics in this study were prepared using MacPyMOL (Schrödingeret al., 2015).

2.7 Cell viability assay

Molecular Pharmacology Fast Forward. Published on October 8, 2020 as DOI: 10.1124/molpharm.120.000070
This article has not been copyedited and formatted. The final version may differ from this version.

Cells were seeded in a 96-well plate and treated with the indicated concentrations of agents. After 48 h, cell viability was measured by the Cell Titer-Glo luminescent cell viability assay (Promega, Madison, WI, USA). Cell viability is shown as the percentage of the control.

2.8 Detection of apoptotic cells

Cells were seeded in a 96-well plate and treated with the indicated concentrations of agents. After 48 h, nuclei were stained with 10 μg/mL Hoechst 33342 (Thermo Fisher Scientific) for 10 min. Fluorescence images were acquired with the IN CELL ANALYZER 6000. Apoptotic cells were determined by nuclear condensation and fragmentation. The percentage of apoptotic cells was calculated by dividing the number of apoptotic cells by the total number of cells.

2.9 Statistical Analysis

Quantitative results are presented as means ± SD ($n \geq 3$). A two-tailed Student's t-test was used to evaluate the significance of differences between two groups. A value of $p < 0.05$ was considered statistically significant.

Molecular Pharmacology Fast Forward. Published on October 8, 2020 as DOI: 10.1124/molpharm.120.000070
This article has not been copyedited and formatted. The final version may differ from this version.

3. Results

3.1 Identification of GZD824 as a GCN2-ATF4 pathway inhibitor

To evaluate activation of the ISR promptly and quantitatively, we examined expression levels of ATF4 in nuclei by immunofluorescence staining of HT1080 cells (Fig. 1A). Treatments of cells with halofuginone (prolyl transfer RNA synthetase inhibitor) (D'Aniello et al., 2015) and tunicamycin (N-glycosylation inhibitor) (Gahmberg et al., 1980) for 6 h induced nuclear ATF4, which was prevented by siRNAs against *GCN2* and *PERK*, respectively. Thus, we found that halofuginone activated the GCN2 arm of the ISR, whereas tunicamycin activated the PERK arm. Using this system, we screened a kinase inhibitor library (355 compounds at 2 μM each) and identified GZD824 (Fig. S1), a known BCR-ABL inhibitor, which preferentially prevents activation of the GCN2 arm compared with the PERK arm.

Indeed, 2 μM GZD824 prevented ATF4 induction during halofuginone stress, but only marginally during tunicamycin stress in HT1080 cells (Fig. 1B and C). Conversely, GSK2656157, a specific inhibitor of PERK (Atkins et al., 2013), suppressed ATF4 induction under stress conditions caused by tunicamycin, but not halofuginone (Fig. 1C). Immunoblot analysis consistently revealed that GZD824 prevented ATF4 induction under GCN2-activating conditions due to halofuginone addition for 6 h and glutamine withdrawal for 18 h, but not under PERK-activating conditions due to tunicamycin addition for 6 h and glucose withdrawal for 18 h (Fig. 1D and E). In addition, phosphorylation of GCN2 at T899, a marker of activation, was suppressed by GZD824, but it did not affect the phosphorylation status of PERK, as detected by an upward mobility shift. These results demonstrated that GZD824 inhibited activation of the GCN2-ATF4 pathway in the ISR.

Molecular Pharmacology Fast Forward. Published on October 8, 2020 as DOI: 10.1124/molpharm.120.000070
This article has not been copyedited and formatted. The final version may differ from this version.

3.2 Dual effects of GZD824 on ATF4 expression

We next examined the dose-dependent effects of GZD824 on GCN2-ATF4 and PERK-ATF4 pathways. For this purpose, we used histidinol, which mimics amino acid starvation (Zhang et al., 2002), and thapsigargin, a non-competitive inhibitor of sarco/endoplasmic reticulum Ca^{2+} ATPase (Urano et al, 2000), as GCN2- and PERK-activating stressors, respectively. Treatments of HT1080 cells with these stressors for 4 h induced ATF4 as shown by immunofluorescence staining (Fig. 2A and B). In agreement with the above results, the ATF4 induction by histidinol, but not thapsigargin, was inhibited by GZD824 in a dose-dependent manner at concentrations ranging from 0.1 to 1 μM. Furthermore, immunoblot analysis revealed that GZD824 dose-dependently suppressed phosphorylation of GCN2 and induction of ATF4 under histidinol stress (Fig. 2C). These results further showed that GZD824 preferentially inhibited activation of the GCN2-ATF4 pathway of the ISR.

During the above examination, we found that GZD824 by itself induced ATF4 expression under normal conditions, peaking at 0.1 μM and attenuating at higher concentrations of 0.3 and 1 μM (Figures S2, 2A–C). The ATF4 induction by 0.1 μM GZD824 in HT1080 cells occurred with a slight increase in phosphorylation of eIF2α S51, but without an increase in phosphorylation of GCN2 T899 (Fig. 2D). In fact, GCN2 phosphorylation was rather decreased by treatment with GZD824. Essentially the same results were obtained using NCI-460 and A549 cells (Fig. 2D). Taken together, GZD824 at low concentrations (~0.1 μM) induced ATF4 expression under normal conditions, but at higher concentrations (0.3–1 μM), it prevented ATF4 induction under GCN2-activating stress conditions.

Molecular Pharmacology Fast Forward. Published on October 8, 2020 as DOI: 10.1124/molpharm.120.000070
This article has not been copyedited and formatted. The final version may differ from this version.

3.3 GCN2 kinase as a direct molecular target of GZD824

Although somewhat paradoxically, impeding GCN2 arm activation by GCN2 knockdown impaired ATF4 induction in HT1080 cells treated with 0.1 μM GZD824 for 4 h (Fig. 3A). Thus, a low concentration of GZD824 induced ATF4 likely through a GCN2-dependent mechanism. In line with this finding, such a paradoxical effect of GZD824 on ATF4 expression was recapitulated using GCN2iB, a potent ATP-competitive GCN2 kinase inhibitor that has been reported recently (Nakamura et al., 2018). Indeed, similar to GZD824, GCN2iB elicited ATF4 induction with slightly increased eIF2α phosphorylation at a low concentration of 0.1 μM, although it reduced GCN2 phosphorylation dose-dependently in the range of 0.1–1 μM (Fig. 3B). The GCN2iB-elicited ATF4 induction was also impaired by GCN2 knockdown (Fig. 3A). However, unlike GZD824 and GCN2iB, BCR-ABL inhibitors imatinib and dasatinib (Weisberg et al., 2007) had almost no effect on ATF4 expression or GCN2/eIF2α phosphorylation in HT1080 cells under both normal and stress conditions (Fig. 3C). Thus, in regard to the effects on GCN2-related signaling pathways, GZD824 shared similar properties with GCN2iB rather than BCR-ABL inhibitors.

We next compared the effects of GZD824, GCN2iB, and dasatinib on GCN2 kinase activity in an *in vitro* kinase assay consisting of recombinant human GCN2 (192-1024) and eIF2α (full length) proteins (Fig. 3D). After incubation with these drugs at graded concentrations in the range of 0.001–1 μM, GCN2 kinase activity was assessed by phosphorylation levels of eIF2α S51. In this assay system, GZD824 and GCN2iB similarly inhibited GCN2 kinase activity at 0.1 and 1 μM, but they rather enhanced the activity at 0.001 μM. In contrast, dasatinib did not elicit such dose-dependent effects, although it slightly inhibited GCN2 kinase activity. Docking analysis illustrated that

Molecular Pharmacology Fast Forward. Published on October 8, 2020 as DOI: 10.1124/molpharm.120.000070
This article has not been copyedited and formatted. The final version may differ from this version.

GZD824 was accommodated by the inhibitor binding pocket of the GCN2 kinase (Fig. 3E). These results suggest that, similar to GCN2iB, GZD824 acts on GCN2 directly and elicits biphasic effects on GCN2 kinase activity depending on the concentration.

3.4 Cellular sensitization to GCN2-activating stress by GZD824

To examine cellular sensitivity to GZD824, we treated HT1080 cells with this drug (0.5–1 μM) for 48 h, in combination with amino acid deprivation-mimicking stressors histidinol and halofuginone. GZD824 alone slightly inhibited cell growth, but it showed a more potent growth inhibitory activity in the presence of either histidinol or halofuginone (Fig. 4A). The combination of GZD824 and histidinol clearly enhanced apoptosis induction as determined by nuclear fragmentation (Fig. 4B). Similarly, GCN2iB prevented ATF4 induction and reduced cell viability during histidinol stress, although GCN2iB itself had almost no cytotoxicity (Fig. S3). These results suggested that GZD824 sensitized HT1080 cells to amino acid starvation stress, possibly by inhibiting the GCN2 arm of the ISR similarly to GCN2iB.

To examine the effects of combined treatment with GZD824 and histidinol in other cell lines, we used NCI-H460 and A549 cells. In both cell lines, GZD824 effectively prevented phosphorylation of GCN2/eIF2α and induction of ATF4 under 4 h-histidinol stress (Fig. 5A). When both cell lines were treated with GZD824 alone for 48 h, similar growth inhibition was observed (Fig. 5B and C). However, sensitization by the combination of GZD824 and histidinol was only seen in NCI-H460 cells, but not A549 cells. The precise reason remains unknown, but the lack of the sensitizing effect of GZD824 might be related to the fact that A549 cells exhibited intrinsically higher sensitivity to histidinol than NCI-460 and HT1080 cells. Taken together, sensitization to

Molecular Pharmacology Fast Forward. Published on October 8, 2020 as DOI: 10.1124/molpharm.120.000070
This article has not been copyedited and formatted. The final version may differ from this version.

amino acid starvation stress by GZD824 was observed in a manner dependent on the cell type.

3.5 Cellular sensitization to GCN2-activating stress by ATF4 knockdown

In HT1080 and NCI-460 cells where GZD824 elicited stress vulnerability, we examined the effects of ATF4 induction on cellular sensitivity to histidinol. For this purpose, we knocked down ATF4 expression in HT1080 and NCI-460 cells using two different types of siRNAs specific for *ATF4* (Fig. 6A and S4A). Although ATF4 knockdown alone for 48 h had little effect on cell viability except in one experimental set, combined treatment with histidinol led to more potent growth inhibition of HT1080 and NCI-H460 cells (Fig. 6B and S4B). Thus, ATF4 contributed to cell survival during histidinol stress, suggesting that prevention of ATF4 induction plays an important role in GZD824-induced stress vulnerability.

Molecular Pharmacology Fast Forward. Published on October 8, 2020 as DOI: 10.1124/molpharm.120.000070
This article has not been copyedited and formatted. The final version may differ from this version.

4. Discussion

We found that GZD824 effectively prevents activation of the GCN2-ATF4 pathway during amino acid starvation stress. GZD824, also known as HQP1351, is an orally available multi-kinase inhibitor that inhibits imatinib-resistant, mutated BCR-ABL and KIT tyrosine kinases. Based on these activities, GZD824 is currently in clinical trials for chronic myelogenous leukemia and in a preclinical development stage for gastrointestinal stromal tumors (Jiang et al., 2018; Liu et al., 2019). However, it is unlikely that the inhibitory activity against BCR-ABL and KIT tyrosine kinases may be involved in the GCN2 pathway inhibition of the cancer cells in this study. Rather, our *in vitro* kinase assay revealed that GZD824 inhibits GCN2 kinase activity as potently as GCN2iB, a recently identified, potent, selective GCN2 inhibitor (Nakamura et al., 2018; Fujimoto et al., 2019). Our results also indicated that GZD824 sensitizes certain cancer cells to amino acid starvation stress, possibly by inhibiting GCN2-elicited ATF4 induction. Thus, GZD824 can be considered as a multi-kinase inhibitor targeting GCN2.

The GCN2-ATF4 pathway promotes cell survival under nutrient-insufficient settings of the tumor microenvironment and plays a major role in tumor growth (Ye, et al., 2010). However, the importance of this pathway for cell survival varies depending on the cell and stress types (Ye et al., 2010; Nakamura et al., 2018), as also observed in this study (Figs. 4 and 5). Therefore, to evaluate the potential of the GCN2-ATF4 pathway as a therapeutic target, GCN2 inhibitors would be useful. In fact, identification of the selective GCN2 inhibitor GCN2iB led to the discovery of a synthetic lethal interaction between GCN2 inhibition and asparagine deprivation in a certain type of cancer cell line (Nakamura et al., 2018). Compared with GCN2iB, GZD824 has a different class of chemical structure and inhibits a different, broad spectrum of kinases

in addition to GCN2 (Ren et al., 2013). These distinctive features of GZD824 might be useful to discover novel synthetic lethal interactions and widening the potential of the GCN2-ATF4 pathway as a therapeutic target.

It is likely that GZD824 and GCN2iB both paradoxically activate GCN2 at lower concentrations than those that inhibit the GCN2-ATF4 pathway effectively. In fact, low concentrations of GZD824 induced eIF2α phosphorylation and ATF4 expression in a GCN2-dependent manner in cells under normal nutrient conditions and induced eIF2α phosphorylation in our *in vitro* GCN2 kinase assay system (Figs. 2 and 3). These were phenocopied by GCN2iB (Fig. 3) that has been reported to inhibit GCN2 most profoundly among 468 kinases examined (Nakamura A, et al., 2018). Therefore, these observations suggest that the paradoxical activation of GCN2 stems from, if not all, the on-target effect of these inhibitors. In this regard, it should be noted that, in contrast to eIF2α phosphorylation and ATF4 induction, T899 autophosphorylation of GCN2 was decreased conversely by low concentrations of GCN2 inhibitors (Figs. 2 and 3). This observation might support the notion that partial inhibition of GCN2 kinase activity occurs during GCN2-eIF2α-ATF4 pathway activation in cells treated with low concentrations of GCN2 inhibitors.

So far, GCN2 activation in cell-free systems has been shown to occur by binding of uncharged tRNA and recently to occur by interactions with ribosomes and the ribosomal P-stalk (Harding et al., 2019). Notably, the latter system indicates that ribosomes stimulate GCN2-dependent eIF2α phosphorylation with no consistent effect on the phosphorylation status of GCN2 T899 (Harding et al., 2019). Thus, it is likely that T899 autophosphorylation of GCN2 is not always a faithful marker for activation of eIF2α-directed kinase activity of GCN2. However, unlike these cell-free systems,

Molecular Pharmacology Fast Forward. Published on October 8, 2020 as DOI: 10.1124/molpharm.120.000070
This article has not been copyedited and formatted. The final version may differ from this version.

neither uncharged tRNA nor ribosomes were added in our *in vitro* system, suggesting that different mechanisms operated in the drug-induced GCN2 activation. Interestingly, a recent study showed that the human GCN2 kinase domain forms a range of conformational states in the presence of ligands bound to the ATP-binding pocket (Maia et al., 2020). Such an unstable nature may raise the possibility that insufficient or partial kinase inhibition by GCN2 inhibitors leads to an active state of eIF2α-directed kinase activity of GCN2. Future studies, especially structural analysis of GCN2 with various GCN2 inhibitors, together with kinetic analysis of the enzymatic activity, will be needed to understand the complicated regulation of GCN2 activity.

In summary, we identified GZD824 as a direct GCN2 inhibitor that prevents activation of the GCN2-ATF4 pathway and sensitizes certain cancer cells to amino acid starvation stress. GZD824 will be useful to elucidate the regulatory mechanisms of GCN2 enzymatic activity and evaluate the potential of the GCN2-ATF4 pathway as a target for cancer therapy. Such information may affect current clinical trials and future clinical development of GZD824.

Molecular Pharmacology Fast Forward. Published on October 8, 2020 as DOI: 10.1124/molpharm.120.000070
This article has not been copyedited and formatted. The final version may differ from this version.

Author contributions

Participated in research design: Kato and Tomida

Conducted experiments: Kato and Takahashi

Contributed analytic tools: Nagasawa and Kunimasa

Performed docking study: Harada and Osawa

Wrote and contributed to writing of the manuscript: Kato, Harada, Osawa, Sugimoto and Tomida

References

Atkins C, Liu Q, Minthorn E, Zhang SY, Figueroa DJ, Moss K, Stanley TB, Sanders B, Goetz A, Gaul N, Choudhry AE, Alsaid H, Jucker BM, Axten JM, Kumar R (2013) Characterization of a novel PERK kinase inhibitor with antitumor and antiangiogenic activity. *Cancer Res* **73**:1993-2002

Dang CV (2012) Links between metabolism and cancer. *Genes Dev* **26**: 877-890

D'Aniello C, Fico A, Casalino L, Guardiola O, Di Napoli G, Cermola F, De Cesare D, Tatè R, Cobellis G, Patriarca EJ, Minchiotti G (2015) A novel autoregulatory loop between the Gcn2-Atf4 pathway and (L)-Proline metabolism controls stem cell identity. *Cell Death Differ* **22**:1094-105

Emsley P, and Cowtan K (2004) Coot: model-building tools for molecular graphics. *Acta Crystallogr D Biol Crystallogr* **60**:2126–2132

Fujimoto J, Kurasawa O, Takagi T, Liu X, Banno H, Kojima T, Asano Y, Nakamura A, Nambu T, Hata A, Ishii T, Sameshima T, Debori Y, Miyamoto M, Klein MG, Tjhen R, Sang BC, Levin I, Lane SW, Snell GP, Li K, Kefala G, Hoffman ID, Ding SC, Cary DR, Mizojiri R (2019) Identification of Novel, Potent, and Orally Available GCN2 Inhibitors with Type 1 Half Binding Mode. *ACS Med Chem Lett* **10**:1498-1503

Gahmberg, CG, Jokinen M, Karhi KK, Andersson LC (1980) Effect of tunicamycin on the biosynthesis of the major human red cell sialoglycoprotein A, in the leukemia cell line K562. *J Biol Chem* **10**:2169-2175

Harding HP, Zhang Y, Zeng H, Novoa I, Lu PD, Calfon M, Sadri N, Yun C, Popko B, Paules R, Stojdl DF, Bell JC, Hettmann T, Leiden JM, Ron D (2003) An integrated stress response regulates amino acid metabolism and resistance to oxidative stress. *Mol Cell* **11**:619-633

Harding HP, Ordonez A, Allen F, Parts L, Inglis AJ, Williams RL, Ron D (2019) The ribosomal P-stalk couples amino acid starvation to GCN2 activation in mammalian cells. *Elife* **8**:e50149

Harding HP, Zhang Y, Bertolotti A, Zeng H, Ron D (2010) Perk is essential for translational regulation and cell survival during the unfolded protein response. *Mol Cell* **5**:897-904

Jiang, Q, Huang, XJ , Chen Z, Men L, Sun X, Jl J, Wang H, Hou Y, Hu P, Zou L, Yan H, Huang Y, Yang D, Zhai Y (2018) Safety and efficacy of HQP1351, a 3rd generation oral BCR-ABL inhibitor in patients with tyrosine kinase inhibitor-resistant chronic myelogenous leukemia: preliminary results of phase I study. ASH Annual Meeting Abstract ID#: 119142

Krissinel E, Henrick K (2004) Secondary-structure matching (SSM), a new tool for fast protein structure alignment in three dimensions. *Acta Crystallogr D Biol Crystallogr* **60**:2256–2268

Liu X, Wang G, Yan X, Qiu H, Min P, Wu M, Tang C, Zhang F, Tang Q, Zhu S, Qiu M, Zhuang W, Fang DD, Zhou Z, Yang D, Zhai Y (2019) Preclinical development of HQP1351, a multikinase inhibitor targeting a broad spectrum of mutant KIT kinases, for the treatment of imatinib-resistant gastrointestinal stromal tumors. *Cell Biosci* **9**: 88

Lu PD, Harding HP, Ron D (2004) Translation reinitiation at alternative open reading frames regulates gene expression in an integrated stress response. *J Cell Biol* **167**: 27-33

Maia de Oliveira T, Korboukh V, Caswell S, Winter Holt JJ, Lamb M, Hird AW, Overman R (2020) The structure of human GCN2 reveals parallel, back-to-back kinase dimer with a plastic DFG activation loop motif. *Biochem J* **477**: 275-284

Nakamura A, Nambu T, Ebara S, Hasegawa Y, Toyoshima K, Tsuchiya Y, Tomita D, Fujimoto J, Kurasawa O, Takahara C, Ando A, Nishigaki R, Satomi Y, Hata A, Hara T (2018) Inhibition of GCN2 sensitizes ASNS-low cancer cells to asparaginase by disrupting the amino acid response. *Proc Natl Acad Sci U S A* **115**: 7776-7785

Qiu H, Gracia-Barrio MT, Hinnebusch AG (1998) Dimerization by translation initiation factor 2 kinase GCN2 is mediated by interactions in the C-terminal ribosome region and the protein kinase domain. *Mol Cell biol* **18**: 2697-711

Quiros PM, Mottis A, Auwerx J (2016) Mitonuclear communication in homeostasis and stress. *Nat Rev Mol Cell Biol* **17**: 213-216

Ren X, Pan X, Zhang Z, Wang D, Lu X, Li Y, Wen D, Long H, Luo J, Feng Y, Zhuang X, Zhang F, Liu J, Leng F, Lang X, Bai Y, She M, Tu Z, Pan J, Ding K (2013) Identification of GZD824 as an orally bioavailable inhibitor that targets phosphorylation and non-phosphorylated breakpoint cluster region-Abelson (Bcr-Abl) kinase and overcomes clinically acquired mutation-induced resistance against imatinib. *J Med Chem* **56**: 879-94

Saito S, Furuno A, Sakurai J, Sakamoto A, Park HR, Shin-Ya K, Tsuruo T, Tomida A (2009) Chemical genomics identifies the unfolded protein response as a target for selective cancer cell killing during glucose deprivation, *Cancer Res* **69**: 4225-4234

Schmidt S, Gay D, Uthe FW, Denk S, Paauwe M, Matthes N, Diefenbacher ME, Bryson S, Warrander FC, Erhard F, Ade CP, Baluapuri A, Walz S, Jackstadt R, Ford C, Vlachogiannis G, Valeri N, Otto C, Schülein-Völk C, Maurus K, Schmitz W, Knight JRP, Wolf E, Strathdee D, Schulze A, Germer CT, Rosenwald A, Sansom OJ, Eilers M, Wiegering A (2019) A MYC-GCN2-eIF2α negative feedback loop limits protein

synthesis to prevent MYC-dependent apoptosis in colorectal cancer. *Nat Cell Biol* **21**: 1413-1424

Schrödinger LLC (2015) The PyMOL molecular graphics system, version. 1.8

Tameire F, Verginadis II, Leli NM, Polte C, Conn CS, Ojha R, Salas Salinas C, Chinga F, Monroy AM, Fu W, Wang P, Kossenkov A, Ye J, Amaravadi RK, Ignatova Z, Fuchs SY, Diehl JA, Ruggero D, Koumenis C (2019) ATF4 couples MYC-dependent translational activity to bioenergetic demands during tumour progression. *Nat Cell Biol* **21**: 889-899

Urano F, Wang X, Bertolotti A, Zhang Y, Chung P, Harding HP, Ron D (2000) Coupling of stress in the ER to activation of JNK protein kinases by transmembrane protein kinase IRE1. *Science* **287**:664-6

Vattem KM, Wek RC (2004) Reinitiation involving upstream ORFs regulates ATF4 mRNA translation in mammalian cells. *Proc Natl Acad Sci U S A* **101**: 11269-11274

Weisberg E, Manley PW, Cowan-Jacob SW, Hochhaus A, Griffin JD (2007) Second generation inhibitors of BCR-ABL for the treatment of imatinib-resistant chronic myeloid leukemia. *Nat Rev Cancer* **7**: 345-56

Ye J, Kumanova M, Hart LS, Sloane K, Zhang H, De Panis DN, Bobrovnikova-Marjon E, Diehl JA, Ron D, Koumenis C (2010) The GCN2-ATF4 pathway is critical for tumour cell survival and proliferation in response to nutrient deprivation. *EMBO J* **29**: 2082-2096

Zhang P, McGrath BC, Reinert J, Olsen DS, Lei L, Gill S, Wek SA, Vattem KM, Wek RC, Kimball SR, Jefferson LS, Cavener DR (2002) The GCN2 eIF2α kinase is required for adaptation to amino acid deprivation in mice. *Mol Cell Biol* **19**: 6681-6688

Zhu J.,Thompson CB (2019) Metabolic regulation of cell growth and proliferation. *Nat Rev Mol Cell Biol* **20**: 436-450

Molecular Pharmacology Fast Forward. Published on October 8, 2020 as DOI: 10.1124/molpharm.120.000070
This article has not been copyedited and formatted. The final version may differ from this version.

Conflict of interest

The authors declare no conflicts of interest.

Acknowledgment

We thank Mitchell Arico from Edanz Group (https://en-author-services.edanzgroup.com/) for editing a draft of this manuscript.

Molecular Pharmacology Fast Forward. Published on October 8, 2020 as DOI: 10.1124/molpharm.120.000070
This article has not been copyedited and formatted. The final version may differ from this version.

Footnotes

This work was supported in part by JSPS KAKENHI Grant Numbers 16H04717, 18K19486 and 19H03526, and the Nippon Foundation.

Molecular Pharmacology Fast Forward. Published on October 8, 2020 as DOI: 10.1124/molpharm.120.000070
This article has not been copyedited and formatted. The final version may differ from this version.

Figure Legends

Fig. 1 Identification of GZD824 as a GCN2-ATF4 pathway inhibitor. (A) HT1080 cells were transfected with siRNA against *GCN2* and *PERK*. Then, the cells were treated for 6 h with halofuginone (HF) and tunicamycin (TM). The cells were fixed and stained with an anti-ATF4 antibody (green) and nuclei were counterstained with Hoechst 33342 (blue) (*left)*. Bars show quantification of the intensity of ATF4 signals in the nucleus. Results are shown as the mean ± SD (n = 3) (*right*). **(B, C)** HT1080 cells were treated for 6 h with 2 μM GZD824 or 100 nM GSK2656157 under normal (Nor) or stress conditions of halofuginone (HF) or tunicamycin (TM). The cells were stained with an anti-ATF4 antibody (green) (data not shown for GSK2656157-treated cells) and the intensities of ATF4 signals were quantified as described in (A). **(D, E)** HT1080 cells were treated for 6 h with 2 μM GZD824 under normal (Nor) or stress conditions due to halofuginone (HF) or tunicamycin (TM) addition (D) and for 18 h with 2 μM GZD824 under normal (Nor) or stress conditions due to glutamine (Gln (-)) or glucose withdrawal（Glc (-)) (E). Cell lysates were subjected to immunoblot analysis with specific antibodies as indicated. $^{**}P < 0.001$, $^{*}P < 0.05$, n.s.: not significant.

Molecular Pharmacology Fast Forward. Published on October 8, 2020 as DOI: 10.1124/molpharm.120.000070
This article has not been copyedited and formatted. The final version may differ from this version.

Fig. 2 Dual effects of GZD824 on ATF4 expression. (A, B) HT1080 cells were treated with 0.1, 0.3, or 1 μM GZD824 for 4 h under normal (Nor) or stress conditions of 2 mM histidinol (His) or 300 nM thapsigargin (TG). After 4 h, the cells were fixed and stained with an anti-ATF4 antibody (green) and nuclei were counterstained with Hoechst 33342 (blue) (A). ATF4 signal intensities were quantified and shown as the mean ± SD (n = 3) (B). **(C, D)** Immunoblot analyses with specific antibodies (as indicated) were carried out using lysates of HT1080 cells treated for 4 h with 0.1, 0.3, or 1 μM GZD824 under normal (Nor) or stress conditions of 2 mM histidinol (His) (C) and lysates of HT1080, NCI-H460, and A549 cells that were treated for 4 h with 0.1 or 1 μM GZD824 or 2 mM histidinol (His) (D). $^{**}P < 0.001$, $^{*}P < 0.05$, n.s.: not significant.

Molecular Pharmacology Fast Forward. Published on October 8, 2020 as DOI: 10.1124/molpharm.120.000070
This article has not been copyedited and formatted. The final version may differ from this version.

Fig. 3 GCN2 kinase as a direct molecular target of GZD824. Immunoblot analyses with specific antibodies were carried out using lysates prepared after cell or purified protein treatments, as follows. **(A)** HT1080 cells were transfected with siRNA against *GCN2* and then treated for 4 h with GZD824 (GZD; 100 nM) (*left*) or GCN2iB (100 nM) (*right*). **(B)** HT1080 cells were treated for 4 h with 0.1 or 1 μM GCN2iB. **(C)** HT1080 cells were treated for 4 h with GZD824, imatinib, or dasatinib at the indicated concentrations under normal (Nor) or stress conditions of 2 mM histidinol (His). **(D)** Recombinant GCN2 protein was preincubated for 60 min with GZD824, GCN2iB, or dasatinib at 0.001, 0.01, 0.1, and 1 μM. Then, the GCN2 proteins were incubated for 3 h with 2 mM ATP and eIF2α recombinant protein. **(E)** Model structure of the GCN2-GZD824 complex. Left: Overview of the model structure. Right: Binding mode of GZD824 and GCN2. Carbon, nitrogen, and fluorine atoms in GZD824 are shown in cyan, blue, and light blue, respectively. GCN2 residues, which appear to be involved in the interaction with GZD824, are shown as sticks. Putative direct interactions are shown by yellow-dotted lines.

Molecular Pharmacology Fast Forward. Published on October 8, 2020 as DOI: 10.1124/molpharm.120.000070
This article has not been copyedited and formatted. The final version may differ from this version.

Fig. 4 Sensitization of HT1080 cells to GCN2-activating stress by GZD824. (A) HT1080 cells were treated for 48 h with GZD824 (GZD) under normal (Nor) or stress conditions of histidinol (His) (*left*) or halofuginone (HF) (*right*). Cell viability was determined by the Cell Titer-Glo Luminescent Cell Viability Assay. Result are shown as the mean ± SD (n = 3). **(B)** After treatments of HT1080 cells with GZD824 under normal (Nor) or stress conditions of histidinol (His; 1 mM) for 48 h, cell nuclei were stained with Hoechst 33342 and observed using an IN CELL ANALYZER 6000. The apoptotic population was calculated and shown by the bar plot. Result are shown as the mean ± SD (n = 3). $^{**}P < 0.001$.

Molecular Pharmacology Fast Forward. Published on October 8, 2020 as DOI: 10.1124/molpharm.120.000070
This article has not been copyedited and formatted. The final version may differ from this version.

Fig. 5 Sensitization of NCI-H460 cells, but not A549 cells, to GCN2-activating stress by GZD824. (A, B) NCI-H460 and A549 cells were treated with GZD824 under normal (Nor) or stress conditions of histidinol [His; 1 mM (NCI-H460) or 0.5 mM (A549)] for 4 h (A) or 48 h (B). After 4 h of treatment, cell lysates were subjected to immunoblot analysis with specific antibodies as indicated (A). After 48 h of treatment, cell viability was determined by the Cell Titer-Glo Luminescent Cell Viability Assay. Result are shown as the mean ± SD (n = 3) (B). $^{**}P < 0.001$, n.s.: not significant.

Molecular Pharmacology Fast Forward. Published on October 8, 2020 as DOI: 10.1124/molpharm.120.000070
This article has not been copyedited and formatted. The final version may differ from this version.

Fig. 6 Cellular sensitization to GCN2-activating stress by ATF4 knockdown. (A, B) HT1080 and NCI-H460 cells were transfected with siRNA against *ATF4* (Ambion SilencerSelect, 5 nM) and cultured under normal (Nor) or stress conditions of 1 mM histidinol (His) for 4 h (A) or 48 h (B). After 4 h of treatment, cell lysates were subjected to immunoblot analysis with specific antibodies as indicated (A). After 48 h of treatment, cell viability was determined by the Cell Titer-Glo Luminescent Cell Viability Assay. Results are shown as the mean ± SD (n = 3) (B). $^{**}P < 0.001$.

Fig. 1

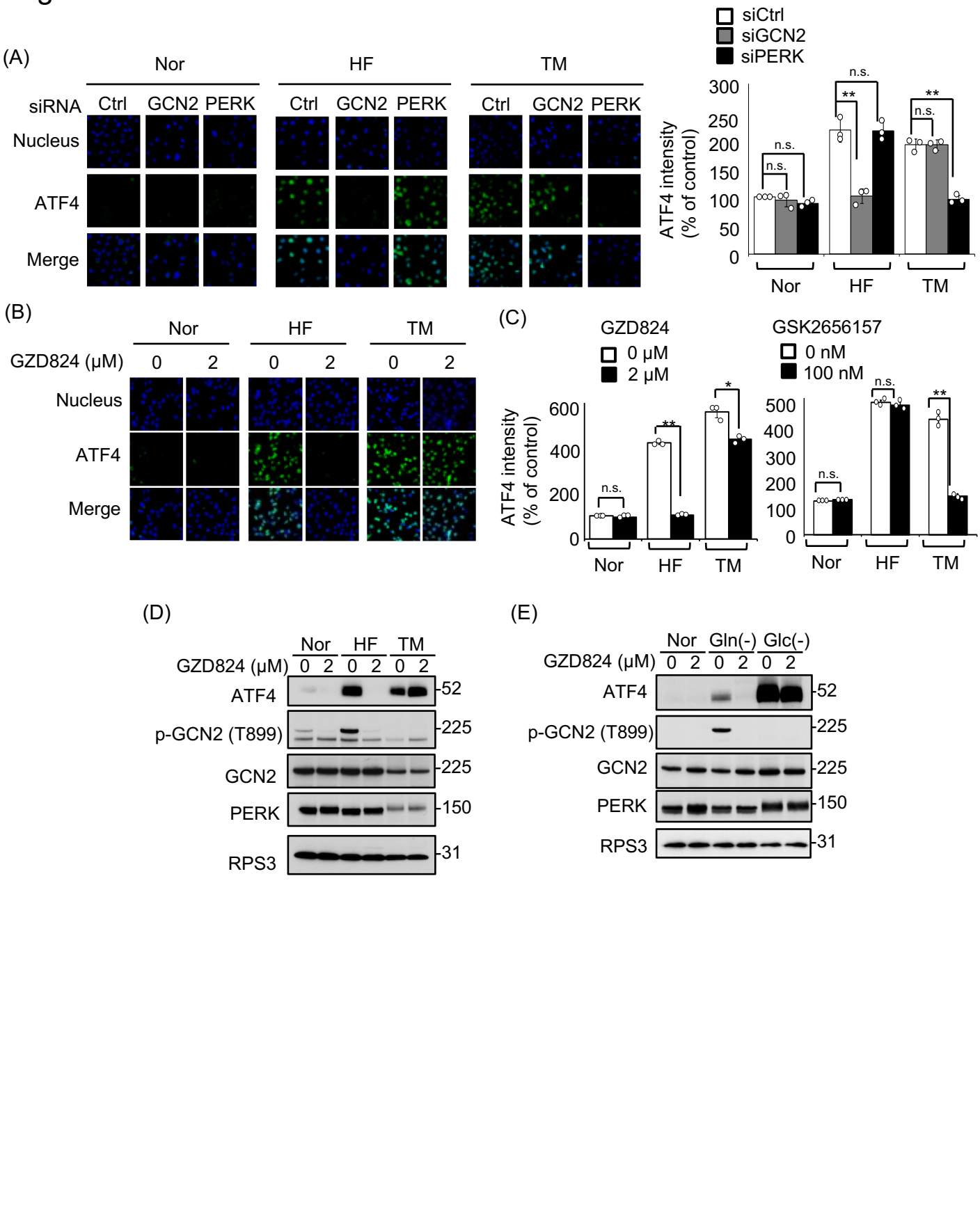
(A)
Nor
HF
TM
siRNA
Ctrl
GCN2
PERK
Nucleus
ATF4
Merge
siCtrl
siGCN2
siPERK
ATF4 intensity (% of control)
n.s.
**
(B)
GZD824 (μM)
0
2
(C)
GZD824
GSK2656157
0 μM
2 μM
0 nM
100 nM
*
(D)
(E)
Gln(-)
Glc(-)
p-GCN2 (T899)
GCN2
PERK
RPS3
52
225
150
31

Fig. 2

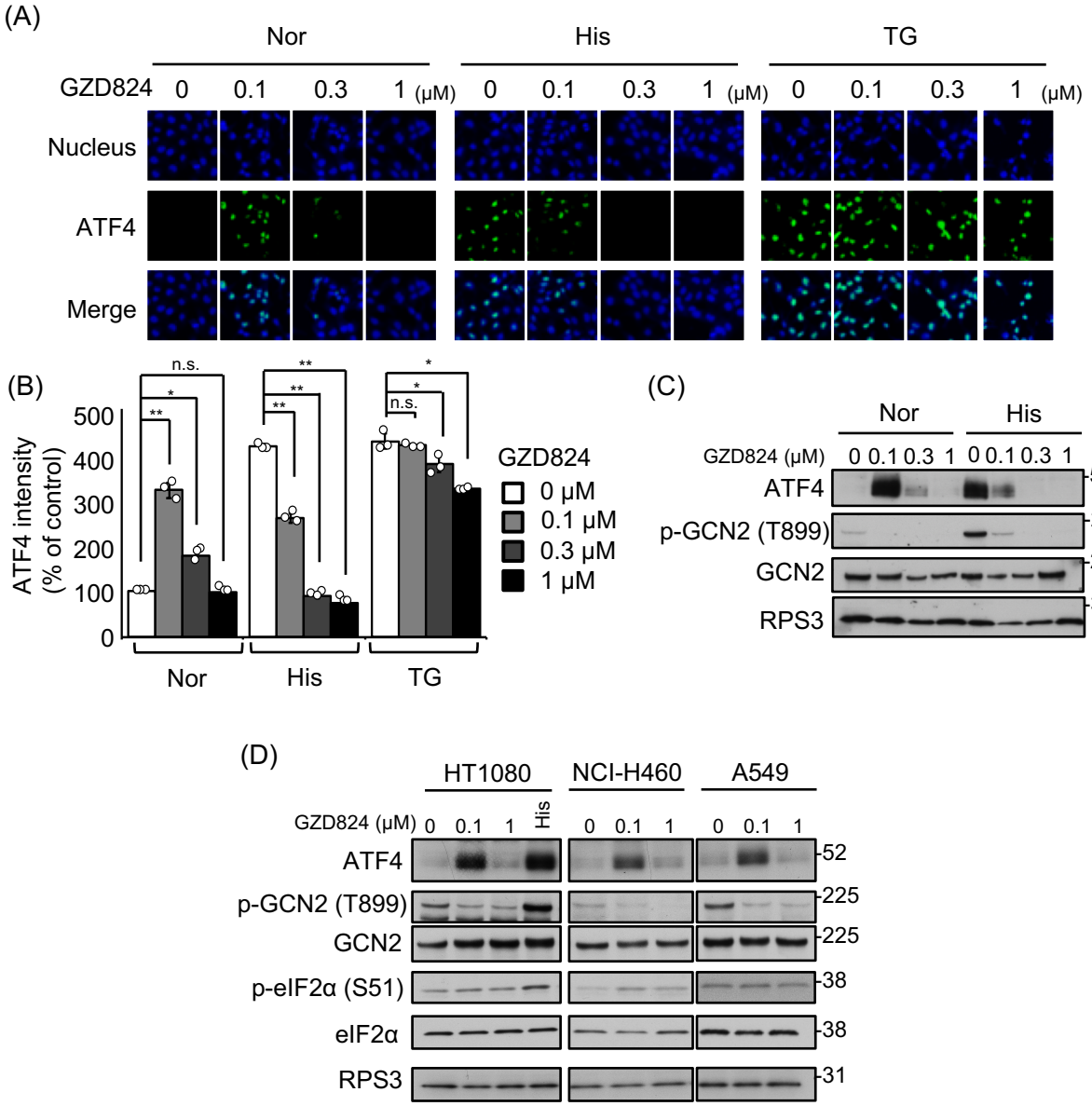
(A)
Nor
His
TG
GZD824 0 0.1 0.3 1 (μM)
Nucleus
ATF4
Merge
(B)
ATF4 intensity (% of control)
500
400
300
200
100
0
n.s.
*
**
GZD824
0 μM
0.1 μM
0.3 μM
1 μM
Nor
His
TG
(C)
Nor
His
GZD824 (μM) 0 0.1 0.3 1 0 0.1 0.3 1
ATF4
p-GCN2 (T899)
GCN2
RPS3
52
225
225
31
(D)
HT1080
NCI-H460
A549
GZD824 (μM) 0 0.1 1 His 0 0.1 1 0 0.1 1
ATF4
p-GCN2 (T899)
GCN2
p-eIF2α (S51)
eIF2α
RPS3
52
225
225
38
38
31

Fig. 3

(A)

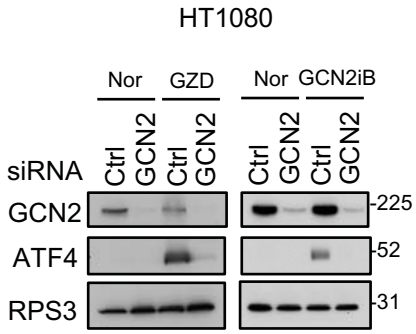

(B)

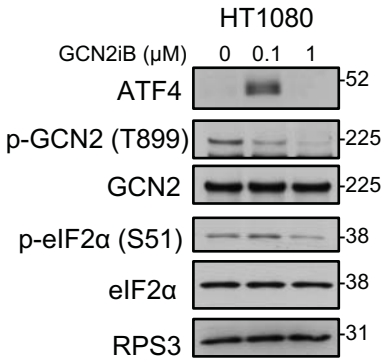

(C)

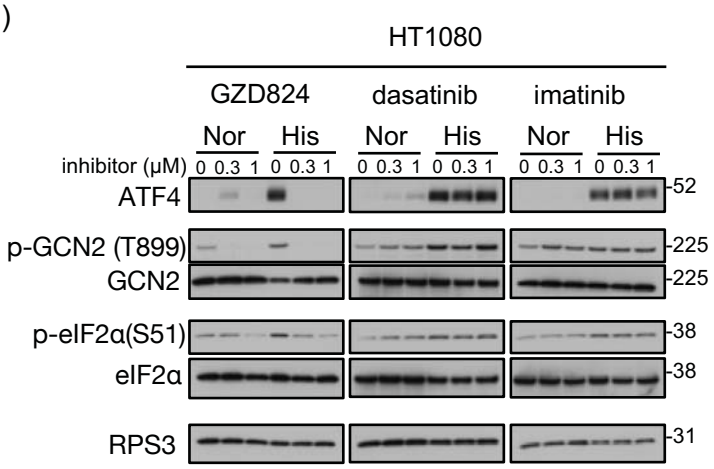

(D)

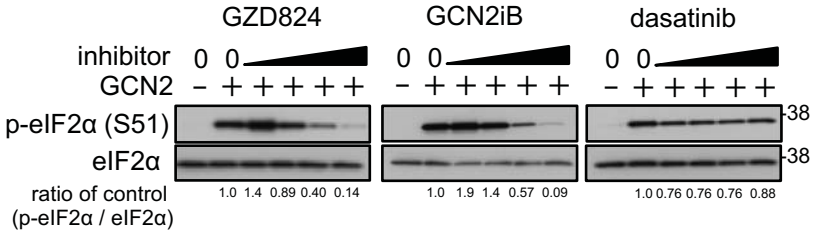

(E)

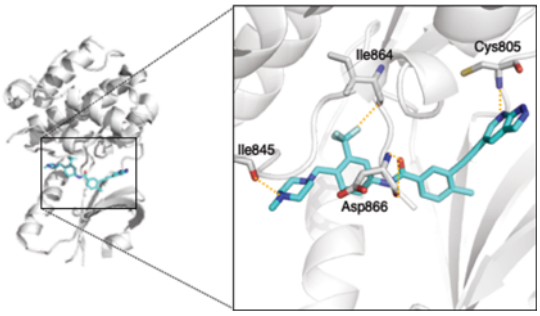

Fig. 4

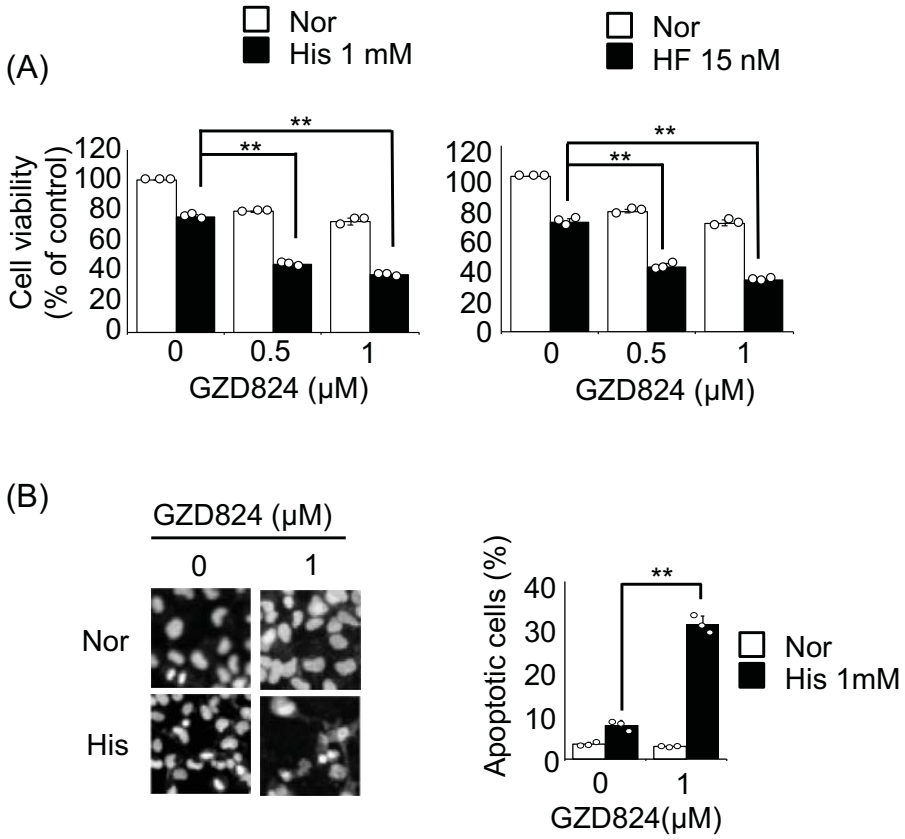

Fig. 5

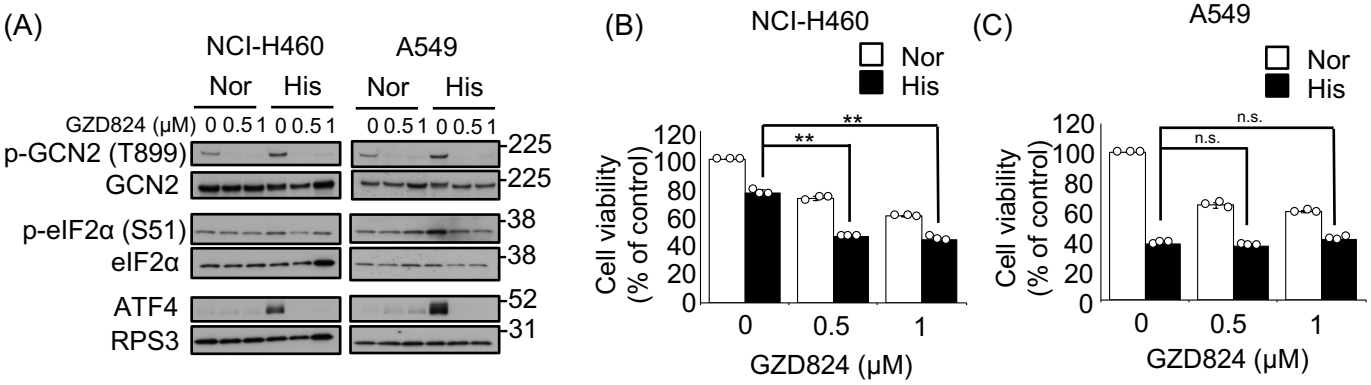
(A)
NCI-H460
A549
Nor
His
Nor
His
GZD824 (μM) 0 0.5 1 0 0.5 1 0 0.5 1 0 0.5 1
p-GCN2 (T899)
GCN2
p-eIF2α (S51)
eIF2α
ATF4
RPS3
225
225
38
38
52
31
(B)
NCI-H460
Nor
His
Cell viability (% of control)
120
100
80
60
40
20
0
**
**
0
0.5
1
GZD824 (μM)
(C)
A549
Nor
His
Cell viability (% of control)
120
100
80
60
40
20
0
n.s.
n.s.
0
0.5
1
GZD824 (μM)

Fig. 6

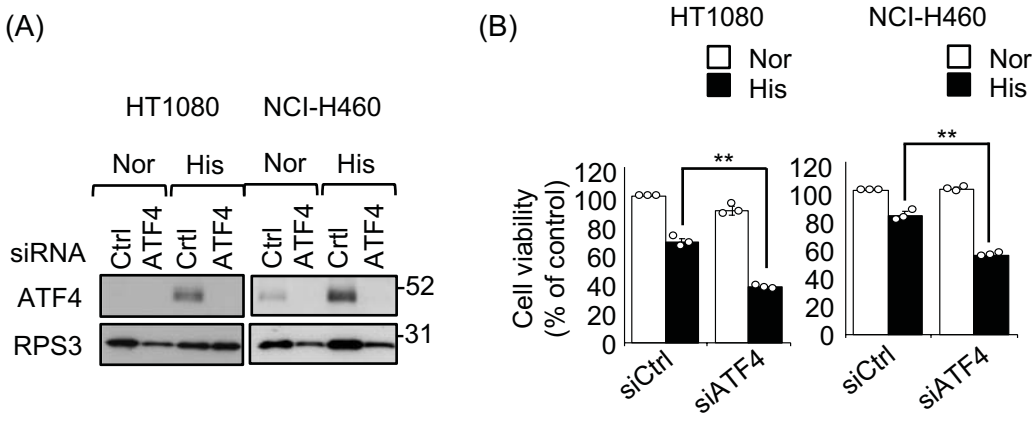

Supplemental data

GZD824 inhibits GCN2 and sensitizes cancer cells to amino acid starvation stress

Molecular Pharmacology 2020.
(MOLPHARM-AR-2020-000070)

Yu Kato, Kazuhiro Kunimasa, Mizuki Takahashi, Ayaka Harada, Ikuko Nagasawa, Masanori Osawa, Yoshikazu Sugimoto and Akihiro Tomida*

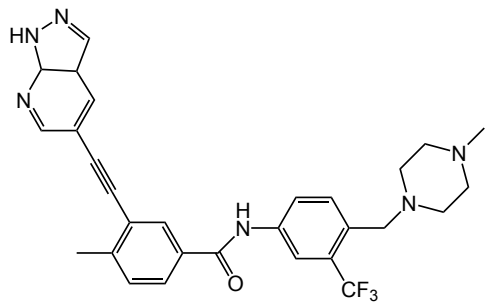

Fig.S1 The structure of GZD824.

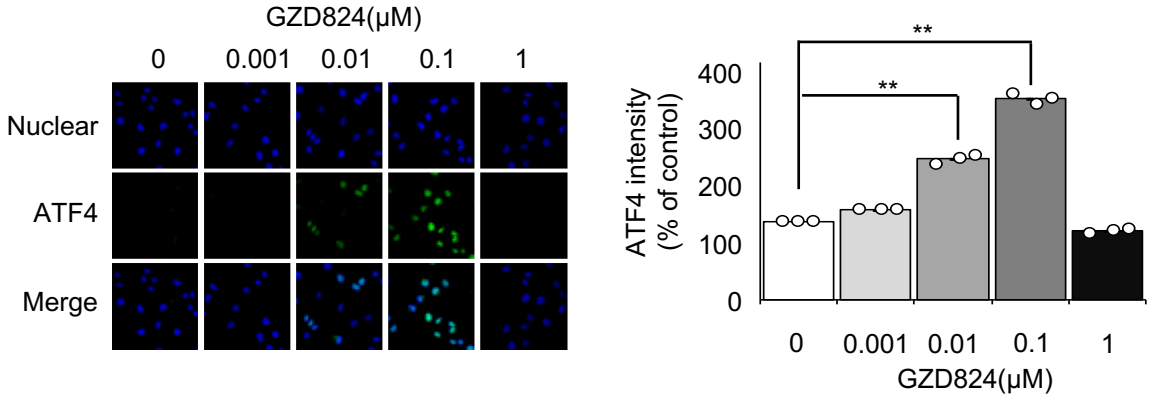

Fig.S2 Dose-dependent effects of GZD824 on ATF4 expression under normal conditions. HT1080 cells were treated for 6 h with 0.001 – 1 μM GZD824 under normal conditions. The cells were fixed and stained with anti-ATF4 antibody (green), and nuclei were counterstained with Hocehst33342 (blue) (*left*) . Quantification of the intensity of ATF4 signals in the nucleus (*right*). Results are shown as the mean ± SD (n = 3). $^{**}P < 0.001$.

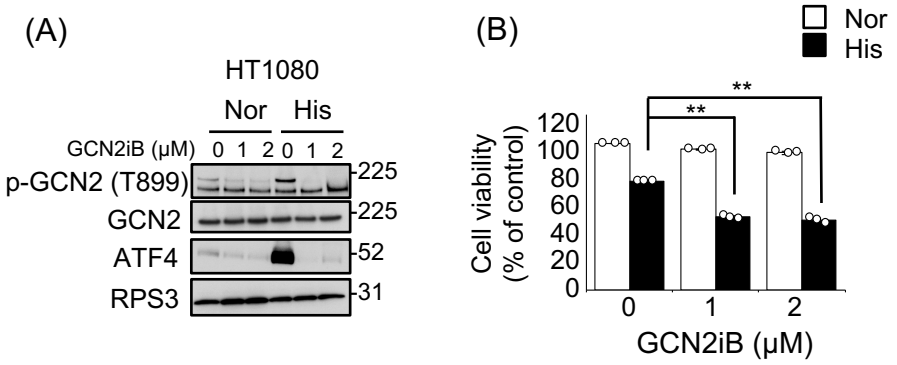

Fig.S3 Effect of GCN2iB on cell viability under amino acid starvation conditions. (A, B) HT1080 were treated with GCN2iB under normal (Nor) or histidinol stress (His). After 4 h treatment, cell lysates were subjected to immunoblot analysis with specific antibodies, as indicated (A). After 48 h treatment, cell viability was determined by the CellTiter-Glo Luminescent Cell Viability Assay. Results are shown as mean ± SD (n = 3) (B). $^{**}P < 0.001$.

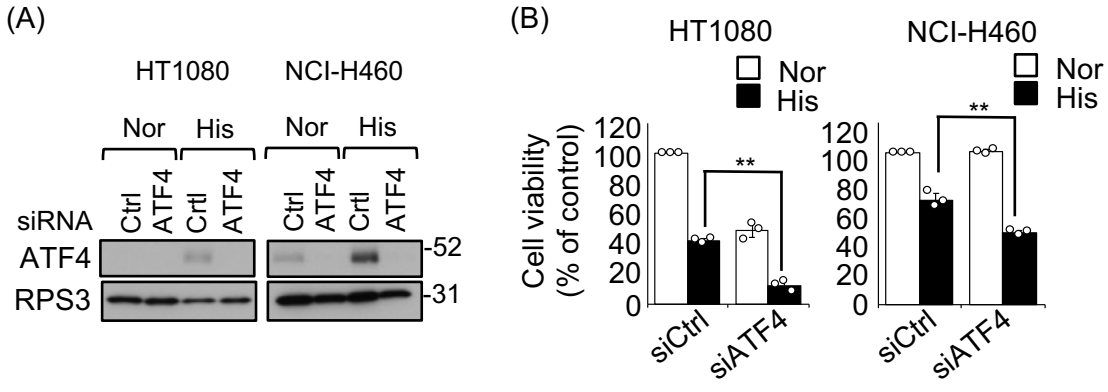

Fig. S4 Silencing *ATF4* sensitizes to amino acid starvation. (A, B) HT1080 and NCI-H460 cells were transfected with siRNA against *ATF4* (Dharmacon ONTARGET Plus, 20 nM) and cultured under normal (Nor) or stress conditions of 1 mM histidinol (His) for 4 h (A) or 48 h (B). After 4 h treatment, cell lysates were subjected to immunoblot analysis with specific antibodies, as indicated (A). After 48 h treatment, cell viability was determined by the CellTiter-Glo Luminescent Cell Viability Assay. Results are shown as mean ± SD (n = 3) (B). $^{**}P < 0.001$.